Pollution, 6(4): 879-892, Autumn 2020
DOI: 10.22059/poll.2020.302442.808
Print ISSN: 2383-451X Online ISSN: 2383-4501
Web Page: https://jpoll.ut.ac.ir, Email: jpoll@ut.ac.ir

Taguchi Optimization of Adsorptive Treatment of Effluent from Lead-acid Battery Recycling unit Using Pressmud-a Sugar Industry Waste

Meshram, S., Thakur, C. * and Soni, A. B.

Department of Chemical Engineering, National Institute of Technology Raipur, 492010, Chhattisgarh, India

Received: 08.05.2020 Accepted: 01.07.2020

ABSTRACT: Lead-acid battery recycling is one of the organized process which helps in overcoming the demand of lead for the production of the storage batteries. During recycling, a large amount of effluent is generated which contains lead beyond the permissible limit and harmful for the environment. This effluent was treated by adsorption as an alternative technique by using another waste (pressmud) as an adsorbent obtained from the sugar industry. Properties of the pressmud were determined through Fourier transform infrared spectroscopy, scanning electron microscope and X-ray diffraction analysis. Taguchi method L16 orthogonal array (4^3) was used for batch adsorption study for the parameters, initial pH, adsorbent dose and contact time. The optimum value for the adsorption of Pb(II) onto pressmud was found at effluent pH 4.5, adsorbent dose 1.0 g/50mL and time 240 min from the Signal-to-Noise ratio analysis. Kinetic and isotherm studies were also carried out to understand the mechanism of adsorption. Langmuir isotherm fitted best to the experimental data with R^2=0.994 and kinetics of adsorption followed the pseudo-second-order model with R^2=0.993.

Keywords: Isotherm, kinetic, lead adsorption, Taguchi analysis.

INTRODUCTION

Lead-acid battery recycling units are the major sources of lead pollutants in the soil which is hazardous to the surrounding communities (Gottesfeld et al., 2018). Recycling of Lead-acid battery is a beneficial process as it not only supplies lead for producing battery but also reduces the pollution. Battery recycling involves the production of the pure lead ingot from exhausted lead electrodes. During the recycling, the electrolyte solution is discharged without treatment by the small recyclers. This effluent of electrolyte solution contains a large concentration (2-300 mg/L) of Pb(II) and it is harmful to the environment and human health (Matlock et al., 2002). This effluent is treated conventionally by neutralization with sodium carbonate, which leads to the generation of a large amount of sludge. However, this method is not effective because the lead hydroxide formed is moderately soluble and remains in the effluent (Dermentzis et al., 2012). According to the Indian Standard Institution, the safe limit of Pb(II) in surface discharge is 0.1 mg/L (Meshram et al., 2020), hence, the effluent must be treated before discharge to the soil or aquatic system to keep the concentration of Pb(II) safe.

Various treatment methods like ion exchange, coagulation, electrocoagulation,

cementation, precipitation, cementation, adsorption have been investigated for the treatment of lead-contaminated water (Calero et al., 2013; Macchi et al., 1993; Volpe et al., 2009; Bahadir et al., 2007). Adsorption is one of the most widely used technique for wastewater treatment, but no work on the adsorptive treatment of effluent of the battery recycling unit has been found in open literature. To make the adsorption more economical, cheap adsorbents like sawdust, bagasse fly ash, pith, rice husk ash, etc. have been investigated as alternative adsorbents for the treatment of wastewater due to high cost of activated carbon (Gupta & Ali, 2004; Thakur et al., 2014; Srivastava et al., 2006; Ayyappan et al., 2005). Pressmud chosen as an adsorbent in this work is a fibrous material obtained as a waste from the sugar industry after the extraction of juice from sugarcane stalks. Usually, it is used as a fertilizer because of nutrients contents. However, with the abundant annual production of pressmud, its disposal is an issue for the sugar industry as well as for the environment (Rondina et al., 2019). Pressmud has been previously used in adsorption by various researchers, Gupta et al. 2012 used the sulphuric acid-treated pressmud to remove cyanide ion; heavy metals were removed from wastewater using a mixture of pressmud-rice husk by Ahmad et al., 2016; pressmud were used as precursor to obtain activated carbon for the removal of methyl orange dye from water by Rondina et al., 2019.

In this study, the effluent of lead-acid battery recycling unit was treated by adsorption using pressmud as adsorbent. Experiments were performed according to the Taguchi method and parameters were optimized for higher adsorption of Pb(II). Langmuir and Freundlich isotherm models and Pseudo-first-order (PFO) and pseudo-second-order (PSO) kinetic models were fitted to the experimental data to understand the mechanism of adsorption.

MATERIAL AND METHODS

Effluents were collected from the local battery recycling unit of Raipur, Chhattisgarh, India. The effluent was found to contain the Pb(II) 11.2 mg/L and it was acidic with pH 1.2. Press-mud was collected from the sugar industry located near Raipur, Chhattisgarh, India. It was dried at a temperature of 90^{o}C then screened to get the uniform size of 1-2 mm and airtight packed for further use.

The Fourier transform infrared spectroscopy (FTIR) spectrum for the wavelength 4000-400 cm^{-1} was obtained using a Bruker, Alpha Model for identification of surface functional groups. The surface micrograph and elemental analysis of the adsorbents before and after the adsorption was obtained by the ZEISS EVO series scanning electron microscope (SEM) Model. The magnification value for the analysis was 500 and 2000. X-ray diffraction (XRD) spectra were obtained to understand the crystalline structure of press-mud by using PANalytical multifunctional XRD analyser. Proximate analysis of the adsorbent was also carried out according to standard ASTM (American Society for Testing and Materials) methods.

Batch adsorption was carried out by taking 50 mL of effluent and a known amount of prepared press-mud in the 250 mL Erlenmeyer flask. The flask was kept in an orbital shaker at 100 rpm for fixed time and temperature. The effluent was then filtered and the concentration of Pb(II) was measured by atomic absorbance spectroscopy (AAS) (Make-Electronics Corporation of India Limited). Percent removal of Pb(II) and adsorbent uptake capacity were determined using Eq. (1) and Eq. (2), respectively.

$$\%\ \text{Removal of } Pb(II) = \frac{C_o - C_e}{C_o} \times 100 \quad (1)$$

$$q_e = \frac{(C_o - C_e)V}{m} \quad (2)$$

where C_o and C_e are the concentration of Pb(II) in the effluent at the initial and at equilibrium, respectively. V is the volume of effluent and m is the mass of adsorbent.

Taguchi method is a simple approach for experimental designs that provides the optimization of experiments and reduces the experimental runs, time and cost (Demirbaş & Yildiz, 2016). This approach helps in determining the effect of parameters, the optimal level of these parameters for the required response, and the relative contribution of each factor (Abou-Shady et al., 2012). This method employs the orthogonal array based on the number of factors and their levels and uses the generic signal-to-noise ratio (SNR) for optimizing the parameters. Signal and noise in the SNR represent the desirable and undesirable values for the response characteristics, respectively (Nandhini et al., 2014). There are three functions for SNR analysis; smaller-the-better, larger-the-better, and nominal-the better. The quality characteristic 'larger-the-better' defined by Eq. (2) was chosen in this study for percent Pb(II) removal and adsorbent capacity (Zolgharnein et al., 2013).

$$\frac{S}{N}_{Larger\text{-}is\text{-}better} = -10 \log\left[\frac{1}{n}\sum_{i=1}^{n}\frac{1}{y_i^2}\right] \quad (3)$$

where y_i denotes n observation of the responses.

Experimental runs were performed in duplicate according to an orthogonal L16 (4^3) array as given in Table 1. Three factors included the parameters, initial pH of effluent (A), adsorbent dose (B) and contact time (C) with four levels. Minitab version 18.1 (2017) trial version was used to design the experiment and optimize the factors for the two responses. An analysis of variance (ANOVA) was done to determine the significance of different parameters.

Table 1. Batch adsorption study factors and their un-coded Levels.

Factor	Name	Level 1	Level 2	Level 3	Level 4
A	pH	1.5	3.0	4.5	6.0
B	Dose, g	0.1	0.4	0.7	1.0
C	Contact time, min	30	60	90	240

RESULTS AND DISCUSSION

FTIR spectra of press-mud before and after adsorption are shown in Fig. 1 for the wavelength 4000-500 cm^{-1}. The figure shows the broad peak at 3420.71 cm^{-1} which could be assigned to both free and hydrogen-bonded OH groups and the stretching peaks at 2920.38 cm^{-1} and 2851.68 can be attributed to silanol groups (Si–OH) and OH groups (methyl radicals), respectively (Gupta et al., 2011). The peak at 1632.90 cm^{-1} may be attributed to –CO and –C–OH groups stretching from ketones and aldehydes and the peak around 1200-1300 cm^{-1} band may be assigned to the aromatic CH and carboxyl-carbonate structures (Gupta et al., 2012). A small peak at 1426.25 cm^{-1} is indicative of -CH_2 and –CH_3 groups (Srivastava et al., 2018). The presence of polysaccharides and lactones can be indicated by the peak at 1043 cm^{-1} which could be assigned to –OCO- and –C-O stretch in alcohols, esters, and ethers (Rout & Arulmozhiselvan, 2019). The peak at 553 cm^{-1} could be due to the Si-H group (Rout & Arulmozhiselvan, 2019). From FTIR analysis it was observed that press-mud contains a significant amount of organic carbon, which could enhance the adsorptive efficiency (Azme & Murshed, 2018). It can be observed that after adsorption intensity of the peaks around 3420 and 2920 cm^{-1} was increased. The peaks at around 1426 and 1258 have been disappeared and the peaks at 1632 and 1043 were shifted to 1641 and 1109, respectively. This shows the involvement surface functional groups like –CH_2, -CH_3, -OCO-, -CO and carboxyl-carbonate structure of the press-mud in adsorption.

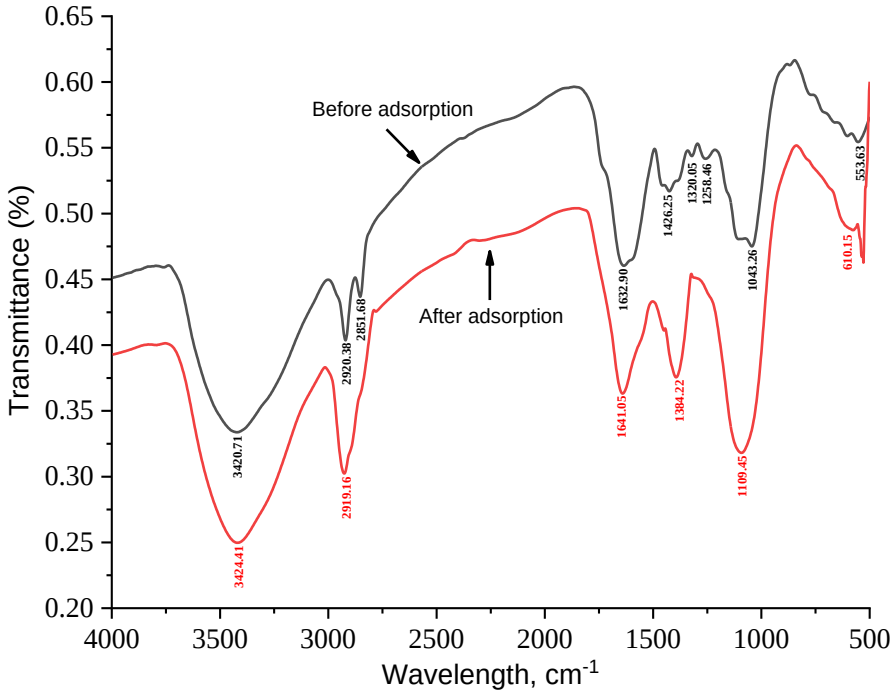

Fig. 1. FTIR spectra of press-mud for the wavelength before and after adsorption.

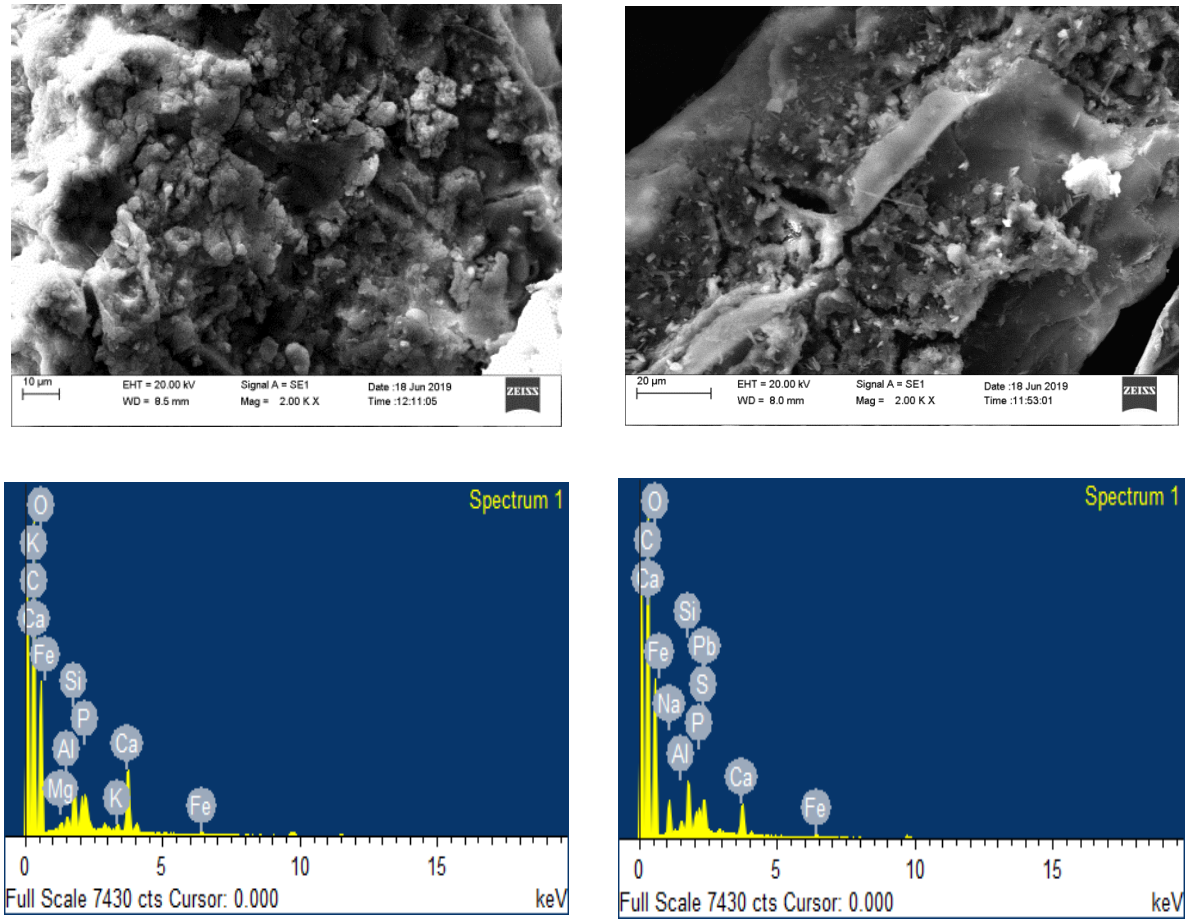

(a) (b)

Fig. 2. SEM and EDS image of press-mud (a) before adsorption and (b) after adsorption.

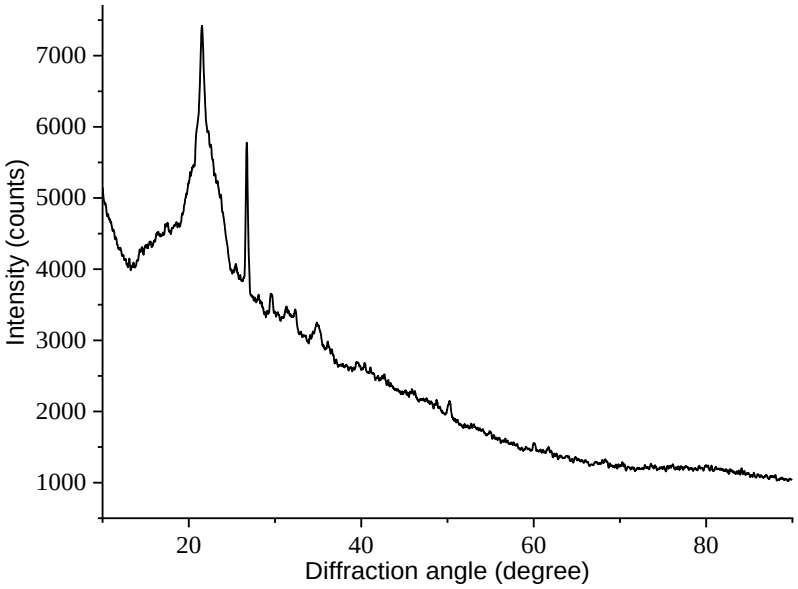

Fig. 3. XRD spectra of press-mud.

Surface morphology of press-mud was determined by SEM analysis after gold coating since press-mud was non-conducting. It can be observed from Fig. 2 that the pressmud has cracked and rough surface. Lead deposition on the surface of pressmud after adsorption is visible. This was also supported by the elemental analysis using Energy-dispersive X-ray spectroscopy (EDX) analysis of pressmud before and after adsorption as presented in Fig. 2 (a) and (b). It can be observed from EDX analysis that the surface of pressmud contains various elements such as calcium, magnesium, silicon, etc. and an extra peak for Pb(II) was found after adsorption. It is also evident from the EDX analysis that elements like sulphur and sodium were also removed from the effluent by the adsorption. The XRD spectra of press-mud (Fig. 3) were compared to the XRD spectra of press-mud found by Gupta et al., 2011 and it was found to contain amorphous silica, ferroaxinite, alumina wairakite, latiumite, mordenite, and calcium-aluminum oxides. Proximate analysis of press-mud was also carried out and it was found to contain fixed carbon 18 %, moisture content 15 %, volatile matter 54 % and ash content 13 %.

According to the Taguchi L16 (4^3) OA, sixteen experiments were performed, and each experiment was repeated twice and the mean values were reported. The value of the responses, percent removal of Pb(II) and adsorbent capacity is illustrated in Table 2. It can be observed from the table that both uptake capacity and percent removal were highest for pH 6.Since the effluent is acidic and it is not economical to maintain the higher pH, so the optimum pH could be chosen as 4. Also for pH 4, the highest uptake capacity was occurred for run 9 due to saturation of available adsorbent dose and maximum percent removal of Pb(II) was occurred for run 12 due to surplus availability of adsorbent dose.

The mean SNR plot for all the factors for percent removal and adsorbent capacity is shown in Fig. 4. According to these figures for uptake capacity, for low adsorbent dose, the SNR increased with increase in pH and the contact time. The largest mean values of SNR were found at A4-B4-C4 for response ‘1’ (percent removal) and at A4-B1-C4 for response ‘2’ (adsorbent capacity). However, the difference in SNR of both responses for levels 3 and 4 of factor A was insignificant

and level 3 could be chosen as the optimum value from an economic point of view. The influences ranking of three factors on the responses are presented in Table 3. It was observed that percent removal was highest for level '4' of all factors. The uptake capacity was highest for level '4' of 'A' and 'C' and level '1' of 'B'. It could also be observed that the pH is the highest influencing factor.

Table 2. L16 orthogonal array of the operational variables, percent removal of Pb(II) and adsorbent capacity.

Exp. No.	A (pH)	B (dose, g)	C (time, min)	% removal	capacity, mg/g
1	1.5	0.1	30	0.63	0.04
2	1.5	0.4	60	0.96	0.01
3	1.5	0.7	90	6.25	0.05
4	1.5	1	240	12.50	0.07
5	3	0.1	60	16.67	0.99
6	3	0.4	30	18.75	0.28
7	3	0.7	240	25.00	0.21
8	3	1	90	35.42	0.21
9	4.5	0.1	90	75.00	**4.47**
10	4.5	0.4	240	96.67	1.44
11	4.5	0.7	30	85.42	0.73
12	4.5	1	60	**98.54**	0.59
13	6	0.1	240	82.08	4.89
14	6	0.4	90	98.33	1.46
15	6	0.7	60	99.17	0.84
16	6	1	30	86.25	0.51

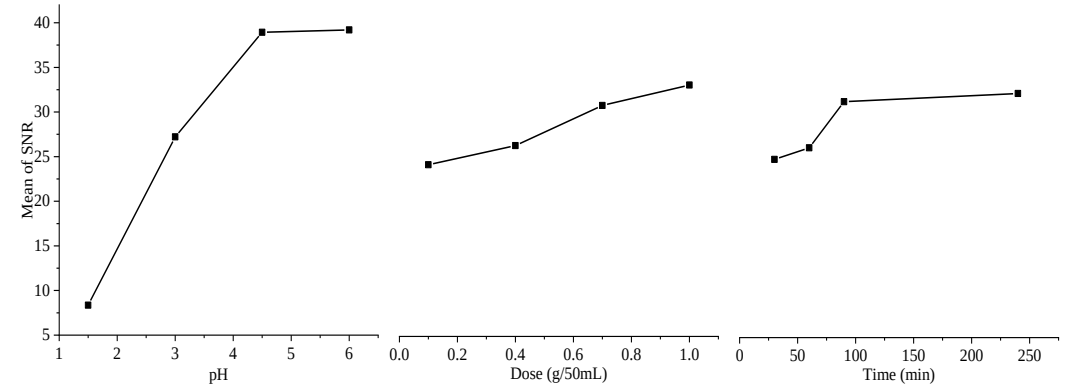

(a)

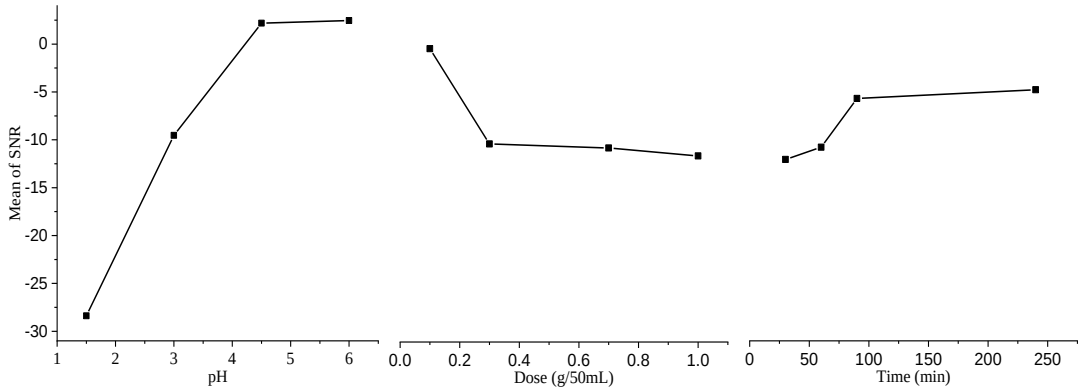

(b)

Fig. 4. Mean SNR for (a) percent removal and (b) adsorbent capacity plotted against different factor levels.

Table 3. Average effect response for SNR on responses.

Factor	A		B		C	
	% R	q	% R	q	% R	q
Level 1	8.351	-28.3867	24.035	-0.4667	24.681	-12.0568
Level 2	27.210	-9.5277	26.162	-10.3806	25.967	-10.7709
Level 3	38.928	2.1898	30.609	-10.7952	31.064	-5.6734
Level 4	39.195	2.4577	32.877	-11.6244	31.972	-4.7658
*Max-min	30.844	30.8445	8.842	11.1577	7.291	7.2910
Rank (R)	1		2		3	
Rank (q)		1		2		3

* Max-min: difference between maximum and minimum value for every column.

ANOVA was performed to investigate the significance and effectiveness of each factor to the responses (Madan & Wasewar, 2017). Tables 4 and 5 show the result of the ANOVA test for the mean response. The *F*-value, the ratio of the mean of squared deviations to mean of squared error, gives the intensity of individual parameter effect on the performance. Generally, a larger *F*-value indicates that the parameter has a larger influence on the output (Ahmad et al., 2018). The Table 4 and 5 indicate that the initial pH of the effluent has the larger effect on Pb(II) removal with *F*-value of 150.60, whereas, for adsorbent capacity, the adsorbent dose was the most effective parameter with *F*-value of 6.15. On the other hand, the adsorption of Pb(II) onto press-mud was least sensitive towards the time of adsorption. It can be observed from Table 4 that R^2 (98.72 %) and adjusted R^2 (96.80 %) are almost similar for the model suggesting that non-significant terms were not present in the empirical model of Pb(II) removal (Yu et al., 2015). It can be observed from table 5 that the adsorbent dose was the most influential factor for adsorbent capacity with *P*-value of 0.029 and the corresponding sum of the squared value of 13.191.

Table 4. Analysis of variance for mean response -%removal of Pb(II).

Source	DF	SS	MS	F-value	P
pH	3	23624.2	7874.73	150.60	0.00001
Dose, g	3	459.9	153.30	2.93	0.122
Time, min	3	112.6	37.54	0.72	0.577
Error	6	313.7	52.29		
Total	15	24510.4			
S	R-sq	R-sq(adj)	R-sq(pred)		
7.23112	98.72%	96.80%	90.90%		

Table 5. Analysis of variance for mean response (adsorbent capacity).

Source	DF	SS	MS	F-Value	P
pH	3	10.969	3.6562	5.12	0.043
Dose, g	3	13.191	4.3969	6.15	0.029
Time, min	3	4.976	1.6586	2.32	0.175
Error	6	4.289	0.7148		
Total	15	33.424			
S	R-sq	R-sq(adj)	R-sq(pred)		
0.845457	87.17%	67.92%	8.75%		

The main effect plot for the percent removal of Pb(II) and adsorbent capacity are shown in Fig. 5. It shows that the percent removal of Pb(II) and adsorbent capacity increased with an increase in the initial pH of effluent. As the pH increases, hydrogen ions decreases and lowers the competition for Pb(II) ions to be adsorbed in the pores of the

adsorbent (Guo et al., 2017). Moreover, at higher pH, deprotonation of surface functional groups of press-mud occurred due to weaker concentration of H^+ in the bulk (Naseem & Tahir, 2001). This deprotonation increases the negative charge on the surface and provides greater electrostatic attraction for Pb(II) and favors the adsorption process (Li et al., 2010). Also, at lower pH, the surface has more H^+ ions thereby it remains unavailable for the Pb(II) ions (Demirbaş & Yıldız, 2016).

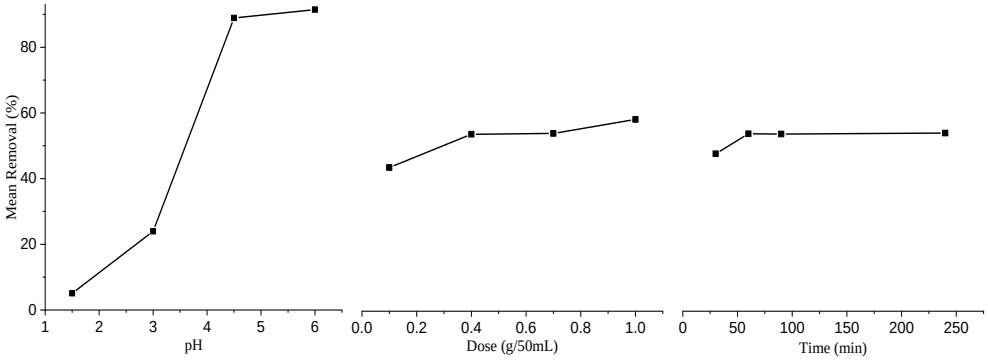

(a)

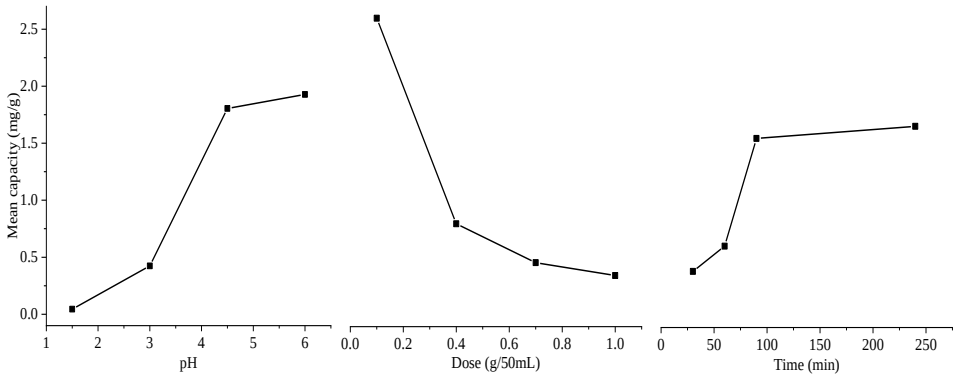

(b)

Fig. 5. (a) Mean removal efficiency and (b) adsorbent capacity plotted against different factor levels.

Fig. 5 illustrates that with the increase in adsorbent dose the percent removal of the Pb(II) increased and adsorbent capacity decreased. The increase in the removal of Pb(II) with adsorbent dose was due to the fact that at higher adsorbent dose large number of adsorption sites were available for adsorption (Demirbaş & Yıldız, 2016). It can also be observed that there was not much difference between the percent removal of Pb(II) at pH 4.5 and 6. So, the pH value of 4.5 was chosen as the optimum pH from the economic point of view. The decrease in the adsorbent capacity with increase in adsorbent dose might be due to the attainment of maximum adsorption at a certain dose and further increase in adsorbent dose resulted in surplus unoccupied adsorption sites (Zolgharnein et al., 2013).

From Fig. 5 (a) and (b), it can be observed that uptake capacity increased with increase in time while the percent removal Pb(II) increased up to 60 min and after that, no significant change occurred. This can be ascribed to the fact that at the start of adsorption large exchangeable sites were available for the occupation of Pb(II) which got saturated with the time leading to more efficient use of press-mud.

The contour plot for the effect of the interaction of two parameters at a time on percent removal Pb(II) and adsorbent

capacity is shown in Fig. 6. For more than 80% removal of Pb(II), the adsorbent dose required was more than 0.6 g/50mL for contact time less than 75 min and at lower adsorbent dose of 0.5 g/50mL, the contact time required was more than 100 min (Fig. 6a). From Fig. 6b and c, it can be noticed that more than 80 % removal was obtained at pH more than 4.2 for all values of adsorbent dose and contact time. High adsorbent capacity was obtained for the adsorbent dose less than 0.1 g/50mL and contact time more than 100 min (Fig. 6d). From Fig. 6e, it is observed that high adsorbent capacity was obtained for pH more than 4.5 and time more than 100 min. From the interaction plot of pH and dose, pH more than 4.5 was required for higher adsorbent capacity when the adsorbent dose was less than 0.2 g/50mL.

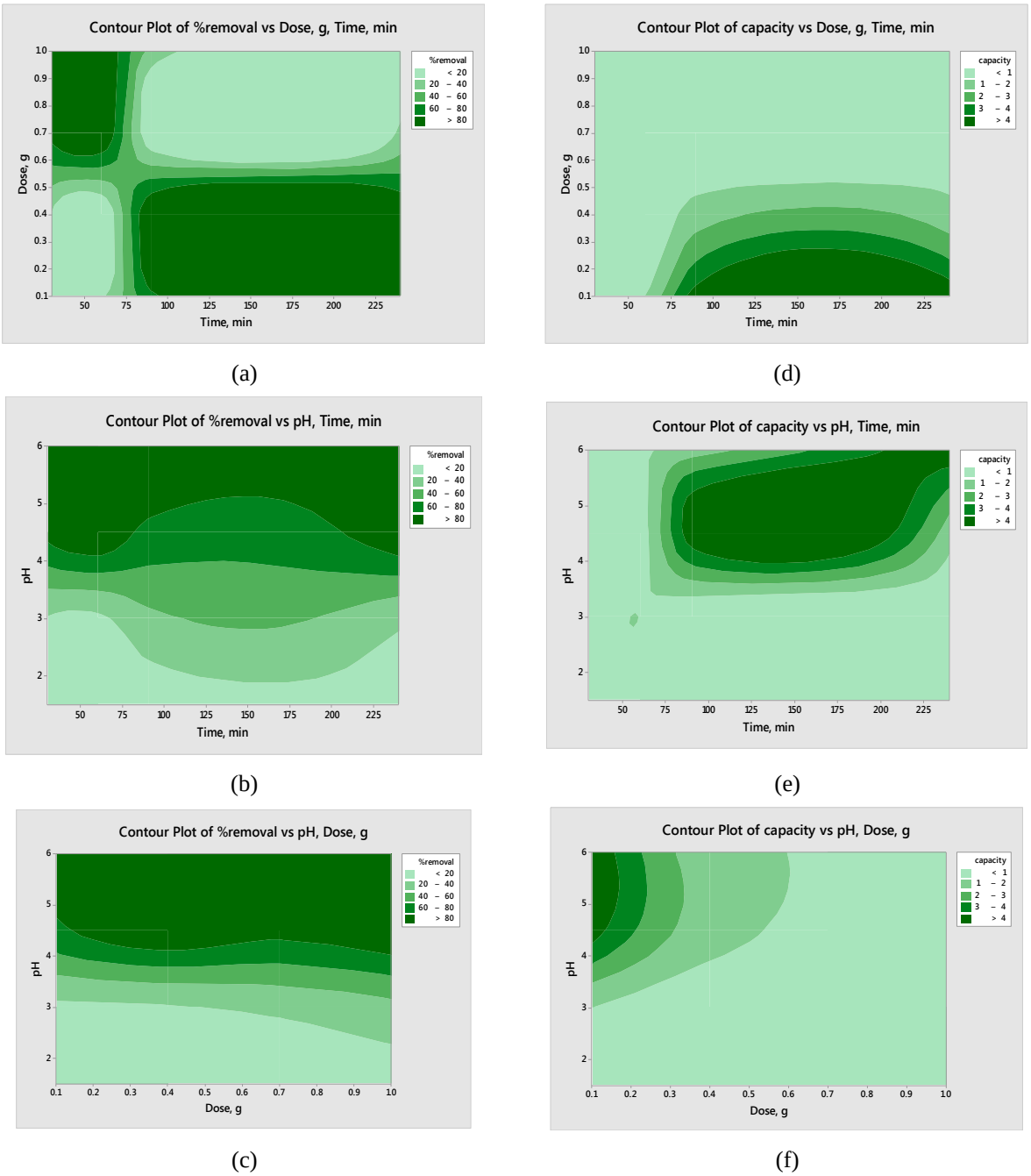

Fig. 6. 2D interaction plot for (a,b,c) percent removal of Pb(II) and (d,e,f) adsorbent capacity.

Langmuir and Freundlich isotherm models were used to understand the mechanism of adsorption of Pb(II) onto press-mud. These two monocomponent isotherms are the most common models to describe the sorption mechanism. Langmuir isotherm is based on the assumption that the adsorption occurs by monolayer adsorption on a homogeneous surface while for Freundlich isotherm metal ion adsorption takes place on a heterogeneous adsorbent surface. The linear equation of the two isotherms are given by Eq.(4) and Eq(5) (Thakur et al., 2016).

$$\frac{C_e}{q_e} = \frac{1}{q_m K_L} + \frac{C_e}{q_m} \tag{4}$$

$$\log q_e = \log K_F + \frac{1}{n} \log C_e \tag{5}$$

where, K_L and K_F are the Langmuir and Freundlich isotherm constant, respectively. q_m is the monolayer adsorbent capacity for Langmuir isotherm and 1/*n* is the intensity of adsorption for Freundlich isotherm. The linear plots of the two models are shown in Fig. 7 and the parameters are reported in Table 6. In this study, Langmuir isotherm fitted well to the experimental data with R^2 value of 0.994. It implies that the adsorption of Pb(II) onto press-mud follows the monolayer adsorption with maximum Langmuir monolayer adsorbent capacity as 3.83 mg/g (Mironyuk et al., 2019). Table 7 shows the uptake capacity of the different adsorbent for the removal of Pb(II). The maximum uptake capacity of press-mud for Pb(II) removal was lower as compared to other adsorbents, which might have because of interference of other dissolved impurities in the effluent. The value of n of Freundlich isotherm was found 1.52, suggesting favorable adsorption and strong interaction between Pb(II) ions and press-mud (Alqadami et al., 2017; Rondina et al., 2019).

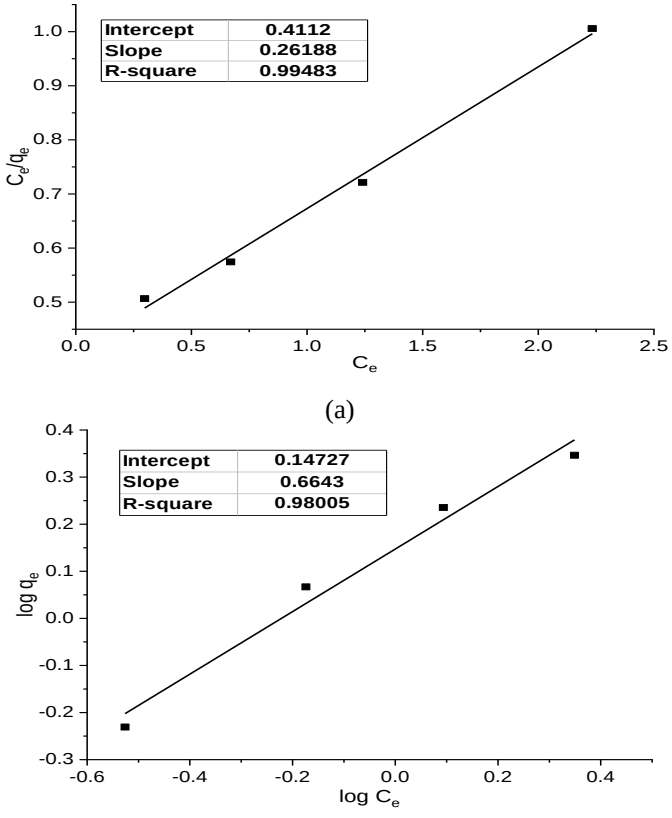

Fig. 7. Linear plot for (a) Langmuir isotherm (b) Freundlich isotherm.

Table 6. Parameters for the Langmuir and Freundlich isotherms.

Langmuir			Freundlich		
$q_{m,}$ mg/g	K_L, L/mg	R^2	n	K_F	R^2
3.831418	3.797372218	0.99483	1.52	1.158353963	0.98005

Table 7. Comparison of different adsorbents for Pb(II) removal.

Adsorbent	Pb(II) Removal, mg/g	Reference
Bagasse fly ash	30	Gupta and Ali 2004
Rhizopus arrhizus	2.643	Bahadir et al. 2007
Malva sylvestris flower	25.64	Salahandish et al. 2016
Papaya peel	38.31	Abbaszadeh et al. 2016
Rice straw nanocelluose	10.20	Kardam et al. 2014
Rice husk nanoadsorbent	6.101	Kaur et al. 2020
Press-mud	3.83	This work

The kinetic study is important to determine the time required to attain the equilibrium and for the prediction of adsorption rate. To study the kinetics two models PFO and PSO were fitted to experimental data. Linear relationships for the two models are shown in Eq. 6 and Eq. 7 (Zhang et al., 2016).

$$\log\left(q_e - q_t\right) = \log q_e - \frac{K_1}{2.303}\left(t\right) \quad (6)$$

$$\frac{t}{q_t} = \frac{1}{K_2 q_e^2} + \frac{1}{q_e} t \quad (7)$$

where q_e and q_t is the metal uptake at equilibrium and at the time (t), respectively. K_1 and K_2 is the rate constant for PFO and PSO kinetic, respectively. The linear plots of the two models are shown in Fig. 8. PFO model assumes that the rate of adsorption is proportional to the number of vacant sites of the adsorbate while PSO is based on the consideration of chemical adsorption as a controlling mechanism (Fajardo et al., 2012). To estimate the kinetic parameters, the models were regressed with the help of experimental data shown in Table 8. The correlation coefficient was found larger for PSO kinetic as compared to that for PFO kinetic. It indicated that the adsorption of Pb(II) ions onto press-mud occurred by chemisorption. Similar results were reported by Gupta and coauthors for the adsorption of cyanide by using press-mud (Gupta et al., 2012).

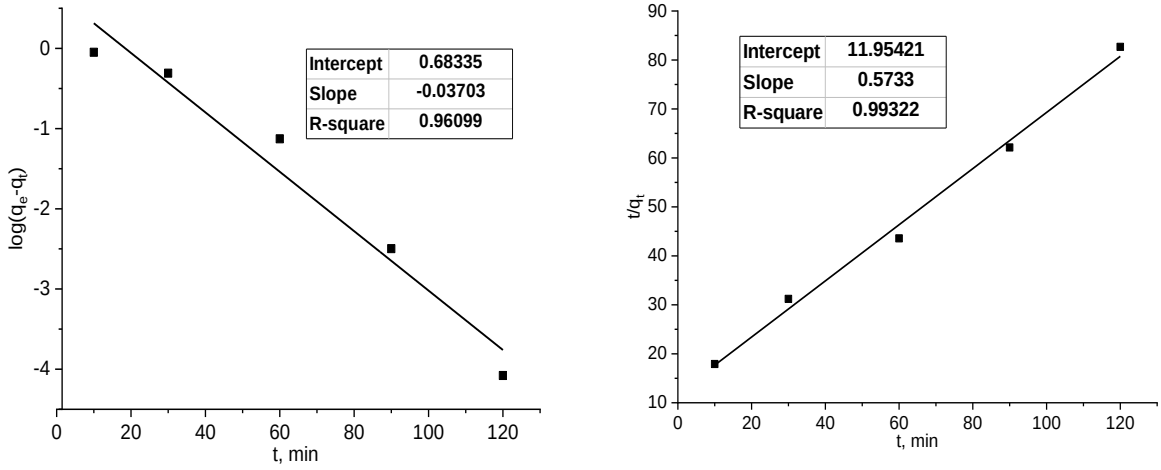

(a) (b)

Fig. 8. Kinetic plot for (a) PFO and (b) PSO model.

Table 8. Parameters of PFO and PSO kinetic models

Pseudo-first order			Pseudo-second order		
K_1, h^{-1}	R^2	q_e, mg/g	K_2, g/mg.h	R^2	q_e, mg/g
0.08528	0.96099	1.980501311	0.027494	0.993	1.744287

CONCLUSION

In this study, the effluent of battery recycling unit was treated by adsorption using press-mud. Experiments were performed according to the Taguchi orthogonal array of L16(4^3). Three factors namely initial pH of the effluent, adsorbent dose, and contact time were chosen each at four levels for the study. Optimum variables were found based on the larger the better SNR. The optimum values were pH 4.5, dose 1.0 g/50mL and 240 min for percent removal of Pb(II) and pH 4.5, dose 0.1 g/50mL and 240 min for uptake capacity. From the result of ANOVA, pH and adsorbent dose were found as the most significant factor for percent removal of Pb(II) and adsorbent capacity, respectively. It was also found that the percent removal of Pb(II) was increased with increase in all the factors. Based on isotherm and kinetic study, it was found that experimental data fitted well to the Langmuir isotherm and PSO kinetic models. This indicated that the Pb(II) adsorption over press-mud was occurred by physical and chemical interaction. The study reveals that press-mud can be utilized for the treatment of the effluent of the battery recycling unit.

ACKNOWLEDGEMENT

Authors are grateful to the Guru Ghasidas Vishwavidyalaya, Bilaspur, Chhattisgarh, India for granting the study leave for Ph.D. program. Authors also want to acknowledge the National Institute of Technology Raipur for providing facilities for the research.

GRANT SUPPORT DETAILS

The present research did not receive any financial support.

CONFLICT OF INTEREST

The authors declare that there is not any conflict of interests regarding the publication of this manuscript. In addition, the ethical issues, including plagiarism, informed consent, misconduct, data fabrication and/ or falsification, double publication and/or submission, and redundancy has been completely observed by the authors.

LIFE SCIENCE REPORTING

No life science threat was practiced in this research.

REFERENCES

Abbaszadeh, S., Alwi, S. R. W., Webb, C., Ghasemi, N. and Muhamad, I. I. (2016). Treatment of lead-contaminated water using activated carbon adsorbent from locally available papaya peel biowaste. J. Clean. Prod., 118; 210-222.

Abou-Shady, A., Peng, C., Bi, J., Xu, H. and Almeria, O. J. (2012). Recovery of Pb (II) and Removal of NO_3^- from Aqueous Solutions Using Integrated Electrodialysis, Electrolysis, and Adsorption Process. Desalination., 286; 304–315.

Ahmad, H., Ee, C. J. and Baharudin, N. S. (2016). A Preliminary Study for Removal of Heavy Metals from Acidic Synthetic Wastewater by Using Pressmud-Rice Husk Mixtures. IOP Conf. Ser.: Earth Environ. Sci., 36; 012031.

Ahmad, S. W., Zafar, M. S., Ahmad, S., Mohsin, M. and Qutab H. G. (2018). Dye Removal from Textile Waste Water Using Potato Starch: Parametric Optimization Using Taguchi Design of Experiments. Arch. Environ. Prot., 44(2); 26-31.

Alqadami, A. A., Naushad, M., Alothman, Z. A. and Ghfar, A. A. (2017). Novel Metal-Organic Framework (MOF) Based Composite Material for the Sequestration of U(VI) and Th(IV) Metal Ions from Aqueous Environment. ACS Appl. Mater. Interfaces, 9(41); 36026–36037.

Ayyappan, R., Sophia, A. C., Swaminathan, K. and Sandhya, S. (2005). Removal of Pb(II) from Aqueous Solution Using Carbon Derived from Agricultural Wastes. Process. Biochem., 40; 1293–1299.

Azme, N. N. M. and Murshed, M. F. (2018). Treatability of Stabilize Landfill Leachate by Using Pressmud Ash as an Adsorbent. IOP Conf. Ser.: Earth Environ. Sci., 140; 012041.

Bahadir, T., Bakan, G., Altas, L. and Buyukgungor, H. (2007). The Investigation of Lead Removal by Biosorption: An Application at Storage Battery Industry Wastewaters. Enzyme Microb. Technol., 41; 98–102.

Calero, M., Pérez, A., Blázquez, G., Ronda, A. and Martín-Lara, M. A. (2013). Characterization of Chemically Modified Biosorbents from Olive Tree Pruning for the Biosorption of Lead. Ecol. Eng., 58; 344–354.

Demirbaş, Ö. and Yıldız, C. (2016). Optimization of Adsorption of Textile Dye onto Diatomite. Asian j. phys. chem. sci., 1(1); 1–9.

Dermentzis, K., Valsamidou, E. and Marmanis, D. (2012). Simultaneous removal of acidity and lead from acid lead battery wastewater by aluminum and iron electrocoagulation. J. Eng. Sci. Technol. Rev., 5(2); 1-5.

Fajardo, A. R., Lopes, L. C., Rubira, A. F. and Muniz, E. C. (2012). Development and application of chitosan/poly(vinyl alcohol) films for removal and recovery of Pb(II), Chem. Eng. J., 183; 253–260.

Gottesfeld, P., Were, F. H., Adogame, L., Gharbi, S., San, D., Nota, M. M. and Kuepouo, G. (2018). Soil Contamination from Lead Battery Manufacturing and Recycling in Seven African Countries. Environ. Res., 161; 609-614.

Guo, Z., Zhang. J., Kang, Y. and Liu, H. (2017). Rapid and Efficient Removal of Pb(II) from Aqueous Solutions Using Biomass-Derived Activated Carbon with Humic Acid in-Situ Modification. Ecotoxicol. Environ. Saf., 145; 442–448.

Gupta, N., Tripathi, S. and Balomajumder, C. (2011). Characterization of Pressmud: A Sugar Industry Waste. Fuel, 90; 389–394.

Gupta, N., Balomajumder, C. and Agarwal, V. K. (2012). Adsorption of Cyanide Ion on Pressmud Surface: A Modeling Approach. Chem. Eng. J., 191; 548–556.

Gupta, V. K. and Ali, I. (2004). Removal of Lead and Chromium from Wastewater Using Bagasse Fly Ash - A Sugar Industry Waste. J. Colloid Interface Sci., 271; 321–328.

Kardam, A., Raj, K.R., Srivastava, S. and Srivastava, M. M. (2014). Nanocellulose fibers for biosorption of cadmium, nickel, and lead ions from aqueous solution. Clean Techn. Environ. Policy, 16; 385–393.

Kaur, M., Kumari, S. and Sharma P. (2019). Removal of Pb (II) from aqueous solution using nanoadsorbent of Oryza sativa husk: Isotherm, kinetic and thermodynamic studies. Biotechnology Reports, 25; e00410.

Li, Y., Du, Q., Wang, X., Zhang, P., Wang, D., Wang, Z. and Xia, Y. (2010). Removal of Lead from Aqueous Solution by Activated Carbon Prepared from Enteromorpha Prolifera by Zinc Chloride Activation. J. Hazard. Mater., 183; 583–589.

Macchi, G., Pagano, M., Santori, M. and Tiravanti, G. (1993). Battery Industry Wastewater: Pb Removal and Produced Sludge. Water Res., 27(10); 1511–1518.

Madan, S. S. and Wasewar, K. L. (2017). Optimization for Benzeneacetic Acid Removal from Aqueous Solution Using CaO_2 Nanoparticles Based on Taguchi Method. J. Appl. Res. Technol., 15; 332–339.

Matlock, M. M., Howerton, B. S. and Atwood, D.A. (2002). Chemical Precipitation of Lead from Lead Battery Recycling Plant Wastewater. Ind. Eng. Chem. Res., 41(6); 1579–1582.

Meshram, S., Thakur, C. and Soni, A. B. (2020). Fixed bed adsorption treatment of effluent of battery recycling unit to remove Pb(II) using steam activated granular activated carbon. J. Serb. Chem. Soc., 84(0); 1-13.

Mironyuk, I., Tatarchuk, T., Naushad, M., Vasylyeva, H. and Mykytyn, I. (2019). Highly Efficient Adsorption of Strontium Ions by Carbonated Mesoporous TiO_2. J. Mol. Liq., 285; 742–753.

Nandhini, M.; Balasubramanian, S.; Ramanujam, S.; Dhakshinamoorthy, G.N. (2014) Optimization of Parameters for Dye Removal by Electro- -Oxidation Using Taguchi Design. J. Electrochem. Sci. Te., 4 (4); 227–234.

Naseem, R. and Tahir, S. S. (2001). Removal of Pb(II) from Aqueous/Acidic Solutions by Using Bentonite as an Adsorbent. Water Res., 35(16); 3982–3986.

Rondina, D. J. G., Ymbong, D. V., Cadutdut, M. J. M., Nalasa, J. R. S., Paradero, J. B., Mabayo, V. I. F. and Arazo, R. O. (2019). Utilization of a Novel Activated Carbon Adsorbent from Press Mud of Sugarcane Industry for the Optimized Removal of Methyl Orange Dye in Aqueous Solution. Appl. Water Sci., 9; 1–12.

Rout, P. P. and Arulmozhiselvan, K. (2019). Investigating the Suitability of Pressmud and Coir Pith for Use as Soilless Substrate by SEM, XRF, UV-Vis and FTIR Spectroscopy Techniques. Cellulose Chem. Technol., 53 (5-6); 599-607.

Salahandish, R., Ghaffarinejad, A. and Norouzbeigi, R. (2016). Rapid and efficient lead (II) ion removal from aqueous solutions using Malva sylvestris flower as a green biosorbent. Anal. Methods, 8; 2515-2525.

Srivastava, V. and Sheth, K. N. (2018). Characterization of Pressmud and Rice Husk Combination for Adsorption of Heavy Metals from Waste Acid Generated from the Processing of E-Waste. Ecol. Environ. Conserv., 24(2); 990-992.

Srivastava, V. C., Mall, I. D. and Mishra, I. M. (2006). Characterization of Mesoporous Rice Husk Ash (RHA) and Adsorption Kinetics of Metal Ions from Aqueous Solution onto RHA. J. Hazard. Mater., 134; 257–267.

Thakur, C., Mall, I. D. and Srivastava, V. C. (2014). Competitive adsorption of phenol and resorcinol onto rice husk ash. Theor. Found. Chem. Eng., 48 (1); 60–70.

Thakur, C., Srivastava, V. C., Mall, I. D. and Hiwarkar, A. D. (2017). Modelling of Binary Isotherm Behaviour for the Adsorption of Catechol with Phenol and Resorcinol onto Rice Husk Ash. Indian Chem. Eng., 59(4); 312-334.

Volpe, M., Oliveri, D., Ferrara, G., Salvaggio, M., Piazza, S., Italiano, S. and Sunseri, C. (2009). Metallic Lead Recovery from Lead-Acid Battery Paste by Urea Acetate Dissolution and Cementation on Iron. Hydrometallurgy, 96; 123–131.

Yu, Y., Chen, N., Hu, W. and Feng, C. (2015). Application of Taguchi Experimental Design Methodology in Optimization for Adsorption of Phosphorus onto Al/Ca-Impregnated Granular Clay Material. Desalin. Water Treat., 56(11); 2994–3004.

Zhang, F., Chen, X., Wu, F. and Ji, Y. (2016). High adsorption capability and selectivity of ZnO nanoparticles for dye removal. Colloids Surf., A : Physicochem. Eng. Aspects, 509; 474–483.

Zolgharnein, J., Asanjarani, N. and Shariatmanesh, T. (2013). Taguchi L16 Orthogonal Array Optimization for Cd (II) Removal Using Carpinus Betulus Tree Leaves: Adsorption Characterization. Int. Biodeterior. Biodegrad., 85; 66–77.